26th International Congress on Modelling and Simulation, Adelaide, SA, Australia, 30 Nov–4 Dec 2025
mssanz.org.au/modsim2025

Simulating Wind-Driven Greenhouse Gas Exchange in Landfills

M. Pjetri [a], **W. Clarke** [a] **and B. Gibbes** [a]

[a] *School of Civil Engineering, The University of Queensland, Australia*
Email: m.pjetri@uq.edu.au

ABSTRACT: Landfill is the dominant source of waste disposal in Australia, constituting 27 % of all solid waste disposed in 2018-2019. Greenhouse gas (GHG) release from landfills can be significant and the quantification of these emissions is a well-established area of investigation. Movement of gases in and out of landfills can be driven by diffusion, changes in atmospheric pressure and gas overpressure from biogenic greenhouse gas production. Another less explored effect is advective exchange driven by wind-induced pressure differentials over the landfill surface.

In this investigation a computational fluid dynamics (CFD) approach was used to assist with the design of laboratory wind tunnel experiments that seek to simulate wind-driven exchange in a porous bedform that is similar to an operational landfill. The modelling and simulation work presented here is part of a broader investigation that aims to explore the significance of this wind-driven exchange process using a combination of numerical modelling and laboratory experiments. A non-traditional method of modelling porous media involving modifying the Navier-Stokes equations with a sink term that accounts for the momentum loss when gas moves through a porous media was used to simulate air flow over bluff bodies representing the landfill and was compared to a typical two-stage modelling approach that involves simulating wind flow over an impermeable bluff body, whose results are later used to model the porous bedform. A model domain that approximated the conditions of the laboratory wind tunnel at The University of Queensland's School of Civil Engineering was created with OpenFOAM. Three different bluff bodies were used to mimic that of a typical landform, namely a trapezoidal prism, a rectangular prism and a semi-cylinder. Each shape was simulated with wind speeds of 1, 2, 5, 10 and 20 $m \cdot s^{-1}$. Both 2D and 3D representations of each shape were tested. Model boundary conditions were set to be equivalent to what was expected to be in the laboratory. An upscaled model was also run for the trapezoidal shape to explore any differences between the two different model scales.

Results indicate pressure gradients at the typical wind speed of 5 $m \cdot s^{-1}$ (and higher) may drive significant exchange within the bedform and external environment. Upscaling from the lab scale to a real-world scale that shows similar pressure gradients as the lab scales may indicate that this process could be a significant driver of exchange in real-world landfills. Results also showed that there was a difference between the wind-driven pressure gradients on the surface of the impermeable bluff body vs the porous bluff body. There was also a difference between the 2D and 3D models for each shape. The upscaled models produced results that had similar flow separation behaviour but had opposite pressure spike behaviour between the impermeable and porous media models compared to the lab scale.

Results suggest that there may be a difference between the behaviour of flow separation over a porous media when it is modelled as an impermeable surface when applying a two-step approach compared to a single step simulation that incorporates porous media using a momentum sink approach. This has important implications for past modelling work that used the two-step approach with an impermeable surface and suggests the surface pressure distribution derived using a CFD approach with impermeable surface might need to be adjusted to better represent the processes associated with wind-driven gas exchange within porous media.

Future work will focus on investigating more complicated landfill geometries that may occur in a real landfill, such as various transitions from concave to convex landforms throughout the operational phase of a landfill.

Keywords: *CFD Modelling, OpenFOAM, Flow-bedform interactions, Porous Media Modelling, Landfills*

1. INTRODUCTION

Landfill is the dominant source of waste disposal in Australia, constituting 27 % of all solid waste disposed in 2018-2019 (Australian Bureau of Statistics, 2020). Greenhouse gas (GHG) release from landfills can be significant and the quantification of these emissions is a well-established area of investigation. In Australia an estimated 2.4 % of total GHG emissions came from landfills (Pickin & Macklin, 2025). Globally, landfill GHG emissions make up 2 % of total GHG emissions (ClimateWatch, 2021). Anthropogenic greenhouse gas emissions are the primary cause of increases in global temperatures in the industrial age (IPCC, 2021).

Movement of gases in and out of landfills (excluding the movement cause by gas extraction wells that are installed in some landfills) can be driven by diffusion, changes in atmospheric pressure and gas overpressure from biogenic greenhouse gas production. Another less explored effect is advective exchange driven by wind-induced pressure differentials over the landfill surface.

In this investigation we use a computational fluid dynamics (CFD) approach to assist with the design of laboratory wind tunnel experiments that seek to simulate wind-driven exchange in a porous bedform that is similar to an operational landfill. The modelling and simulation work presented here is part of a broader investigation that aims to explore the significance of this wind-driven exchange process using a combination of numerical modelling and laboratory experiments.

2. BACKGROUND

Porous media models have been used in conjunction with turbulence models in past work relating river or coastal environment interactions with the bedform (Cardenas & Wilson, 2006; Jin et al., 2010). Porous media in these studies were modelled using Darcy's Law (Cardenas & Wilson, 2006; Gibbes, 2007; Jin et al., 2010) and a modified Richard's equation (Gibbes, 2007) and the turbulent free-surface flows were simulated with a CFD approach based on the Navier-Stokes equations. Both studies modelled the turbulent free surface water flow above the sediments first, assigning the surface of the sediments as a no flow boundary. The resulting surface pressures on the submerged bedforms were then used as the boundary conditions for their porous media flow models. This approach is effectively a one-way sequential coupling of the Navier-Stokes and Richard's equation and does not account for the potential changes in surface pressure distribution as a result of flow out of the bedform (Gibbes, 2007).

A similar approach to modelling the exchange of atmospheric and landfill gases across a landfill surface can assume the air-filled void space in the landfill cover layer is constant and therefore modelled as single-phase fluid flow problem. Constant air-filled void space is assumed in this investigation and therefore the landfill represented as a saturated porous media:

$$S_s \frac{\partial h}{\partial t} = \frac{\partial}{\partial x}(K_x \frac{\partial h}{\partial x}) + \frac{\partial}{\partial y}(K_y \frac{\partial h}{\partial y}) + \frac{\partial}{\partial z}(K_z \frac{\partial h}{\partial z}) \quad (1)$$

Where S_s is the specific storage (m^{-1}), h is the hydraulic head of the fluid (m), K is the hydraulic conductivity in each direction ($m \cdot s^{-1}$) and t is time (s^{-1}).

Another method of modelling porous media involves modifying the Navier-Stokes equations with a sink term that accounts for the momentum loss when gas moves through a porous media (which we call the "momentum-sink approach" throughout the rest of this paper). This type of modelling approach may be extremely useful for modelling computational fluid dynamics with porous media simultaneously. The modification to the Navier-Stokes equations (equation 2) is given by:

$$\rho[\frac{\partial \vec{u}}{\partial t} + \vec{u} \cdot (\nabla \vec{u})] = -\nabla p + \mu \nabla^2 \vec{u} + S \quad (2)$$

Where μ is the dynamic viscosity (Pa·s), $\boldsymbol{u}$ is the velocity of the fluid ($m \cdot s^{-1}$), ρ is the density of the fluid ($kg \cdot m^{-3}$) and ∇ is the gradient operator given by:

$$\nabla = \frac{\partial}{\partial x}\vec{i} + \frac{\partial}{\partial y}\vec{j} + \frac{\partial}{\partial z}\vec{k} \tag{3}$$

where *i, j and k* are the unit vectors is the directions *x*, *y* and *z* respectively. *S* is a momentum sink term given by:

$$S = -(\mu d + \frac{\rho|\vec{u}|}{2} f)\vec{u} \tag{4}$$

where *d* is the Darcy Coefficient (m^{-2}) (which is given by $1/k$, where *k* is the permeability of the porous media (m^2)) and *f* is the Forchheimer Coefficient (m^{-1}) (OpenCFD, 2019). Note that only the momentum equation is modified here as the momentum sink term does not affect the continuity equation. It should also be noted that the flow within the domain is simulated using the Navier-Stokes equations, with the sink term only applied in areas of the domain where porous media is present. The momentum sink approach has not been widely applied to investigate flow in environmental systems, particularly with respect to porous media exchange in response to surface pressure gradients associated with advective flow over fixed bedforms.

In this investigation, we attempt to characterize the differences in these two approaches (traditional two stage approach vs momentum sink approach), with a specific emphasis on determining whether there is a significant difference in the wind-driven surface pressure distribution on the bedform when an impermeable ground surface is simulated compared to the approach that allows air flow within the porous media using the momentum sink approach. The difference between the two approaches will be quantified by comparing the pressures distribution predicted on the surface of the porous media region.

3. METHODOLOGY

A domain that approximated the conditions of the laboratory wind tunnel at The University of Queensland's School of Civil Engineering was created with OpenFOAM. The domain is 2.4 m in the direction of air flow, 0.76 m wide and 0.76 m high, with the bluff body that represents a scaled version of a landfill bedform positioned in the centre of the domain. This is shown below:

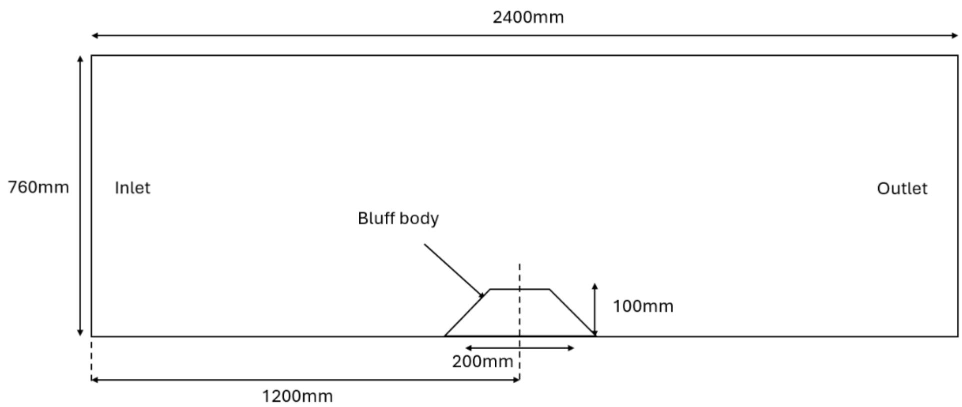

Figure 1 Domain Set-up for proposed laboratory experiments (side view)

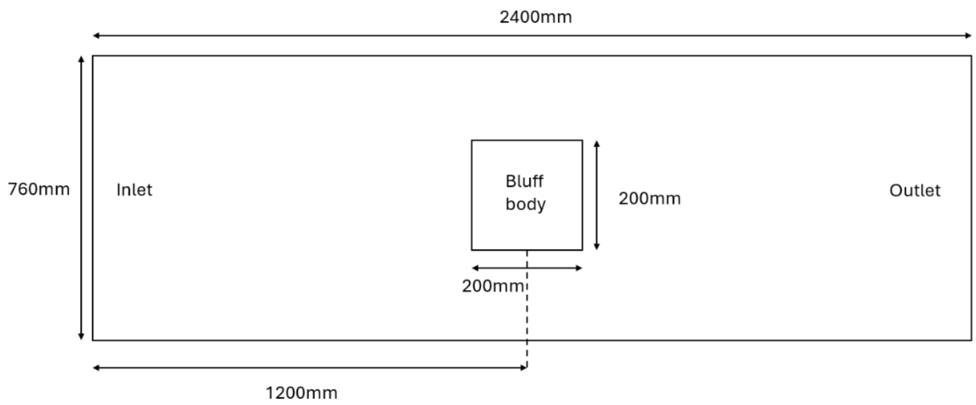

Figure 2 Domain Set-up for proposed laboratory experiments (top view)

The landfill bedform was approximated using a trapezoidal prism, a rectangular prism and a semi-cylinder, with a maximum height of 0.1 m and maximum width of 0.2 m. The effect of modelling the entire domain in two dimensions, the results of which would be validated in the laboratory wind tunnel with a shape that extends the full width of the wind tunnel; or modelling the domain in three dimensions, the effect of which would be validated with a porous media region that only partially extends across the wind tunnel width, is also considered. Wind speeds of 1, 2, 5, 10 and 20 $m{\cdot}s^{-1}$ were simulated, with 20 $m{\cdot}s^{-1}$ representing the maximum wind speed the tunnel can reliably generate. The wind velocity boundary conditions at the inlet were set to a neutral atmospheric boundary condition. This will be adjusted when subsequent laboratory testing begins, and the inlet velocity profile can be measured.

Boundary conditions were set to be equivalent to what is expected to be in the laboratory (except for background pressure, which was set to 0 in the models). The floor of the domain was represented as a no-slip, zero-gradient boundary condition with the top and side walls represented as slip, zero-gradient boundaries. Inlet boundary was set as discussed previously, with the outlet set as a mixed zero-gradient and fixed boundary, which sets the boundary to zero in the case of reverse flow at the boundary.

Initial conditions were set to zero velocity and zero pressure within the domain to make it easier to identify differences in pressure zones and to identify the magnitude of pressures induced by the various wind speeds. A model with atmospheric background pressure as an initial condition was also run to check the validity of initialising the simulations this way, and the pressure distributions and flow behaviour was found to be the same as the zero pressure simulation (with the magnitude of the total pressure being different by exactly the background pressure). Simulations were run for 1500 s, which was sufficient for the simulations to reach a steady-state solution. Mesh density was set such that mesh independence was achieved, with a y+ value within industry guidelines for CFD ($y+ < 5$), ensuring sufficient resolution to accurately describe the boundary layer development.

An upscaled simulation was also run to see if the behaviour is similar in the case of a field scale test. The lab scale geometry and domain were simply increased by a factor of 100 to achieve this (including the atmospheric boundary layer conditions i.e. surface roughness height), with the remainder of the boundary and initial conditions left the same. This was done for the trapezoidal shape, for a typical 5$m{\cdot}s^{-1}$ wind speed.

4. RESULTS/DISCUSSION

The pressure distribution on the surface of the trapezoidal, rectangular and cylindrical shaped bluff bodies for the 5 $m{\cdot}s^{-1}$ inlet wind speed are shown below (Figures 3, 4 and 5). The same set of horizontal co-ordinates are used in all cases to represent each pressure profile.

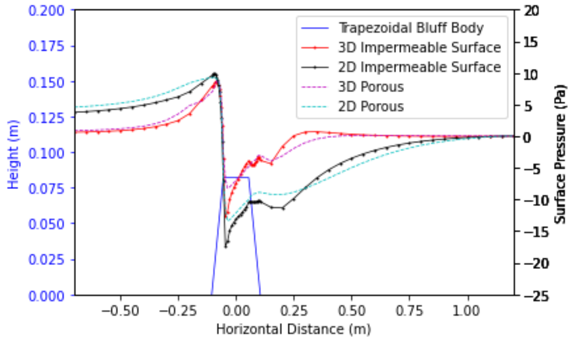

Figure 3 Surface Pressure distributions on a Trapezoidal Bluff Body for 2D and 3D, porous and surface only models for an inlet velocity of 5 m·s^{-1}. Flow here moves from left to right.

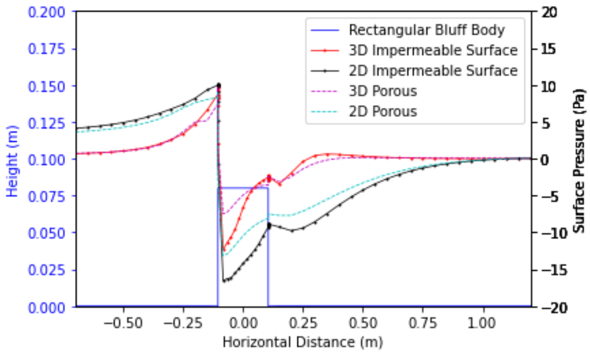

Figure 4 Surface Pressure distributions on a Cubic Bluff Body for 2D and 3D, porous and surface only models for an inlet velocity of 5 m·s^{-1}. Flow here moves from left to right.

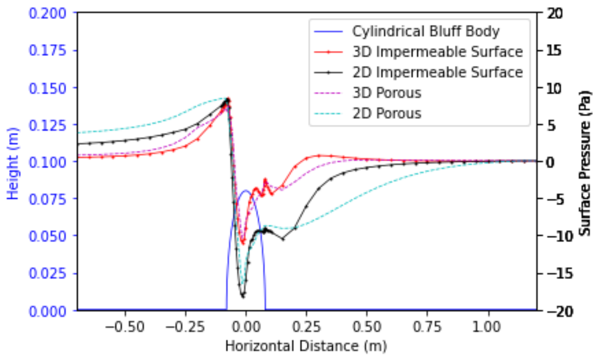

Figure 5 Surface Pressure distributions on a Cylindrical Bluff Body for 2D and 3D, porous and surface only models for an inlet velocity of 5 m·s^{-1}. Flow here moves from left to right.

The pressure distributions in all three shapes follows the characteristic high-pressure zone at the upstream face of the bluff body, followed by low pressure zone at the top, then neutral pressures downstream of the bluff body as expected.

We can also see that for shapes with sharp edges (Figures 3 and 4), there is a large difference (approximately 20 to 29 % increase in the impermeable models) between the porous body and the impermeable body in terms of the sharpness of the change in pressure at the flow separation points. This is due to air flow through the porous media when the bluff body is permeable. Momentum is consequently lost from the air, accounted for in the model by the momentum sink term S. The velocity of air flow is therefore reduced at the point of flow separation and thus a smaller change in pressure at that point. For the cylindrical model (Figure 5) we can see the flow separation occurs further down the shape's surface, likely due to the curved nature of the shape. We also see that the difference in pressure spike between the porous and impermeable models is very small compared to the other two shapes (only 7 to 9% increase in the impermeable models), likely due to the lack of sharp edges in the cylindrical models. Further investigation is required to better understand what is causing this to occur in the cylindrical models.

We can also see that the 2D models have a larger flow separation effect that reattaches further down the model domain. This is as expected, as the 3D representations allow for flow to move around the sides of the model, thus removing energy from the main flow separation that occurs at the front edge of the bluff bodies and allowing flow to reattach further. To check the changes in pressure distributions between wind speeds, the plots below were constructed by normalising the result output by the dynamic pressure at the wind speed.

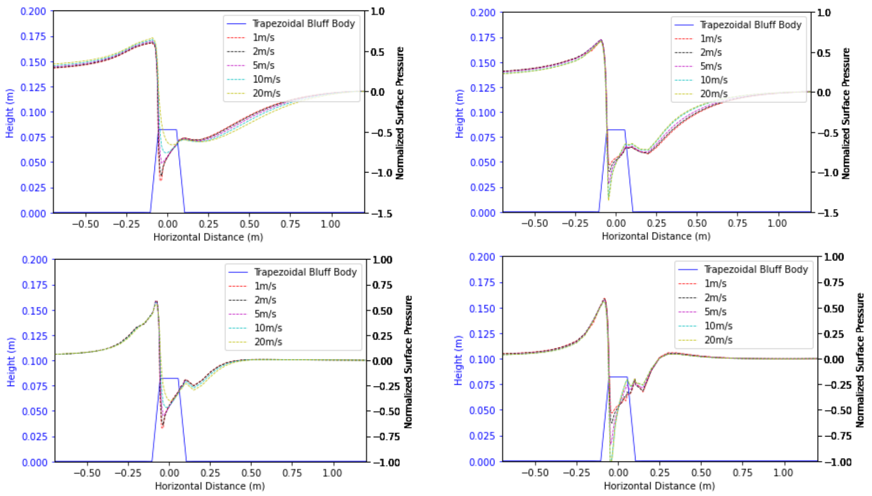

Figure 6 Normalised Pressure distributions for the 2D Porous Model (Top Left), 2D Surface Model (Top Right), 3D Porous Model (Bottom Left) and 3D Surface Model (Bottom Right).

From simulations of the permeable bluff bodies, it is evident that the spike in pressure caused by the sharp edge in the front face of the bedform is softened as the wind speed increases. This is opposite to the behaviour that is seen in the impermeable bluff body models, where an increase in wind speed causes a higher spike at the upstream edge of the bluff body. This difference is likely due to the permeable surface simulations allowing air to flow through the porous media and consequently lose momentum as it flows over the porous media surface. The momentum loss increases with the wind velocity, and thus there is less energy in the pressure spike. From figure 6 we can see the "1m/s" test for the porous media approximates the spike behaviour seen in the surface models, likely due to the slow wind speed not having as much momentum to be drained by the porous media.

Initial experimentation will be used to measure the pressure distributions on permeable and impermeable surfaces of bluff body shapes in the wind tunnel to test whether a permeable porous shape, such as an uncapped landfill in a wind field, does affect the pressure distribution of the surface of that shape as predicted by the model.

The results for the upscaled simulations can be seen below:

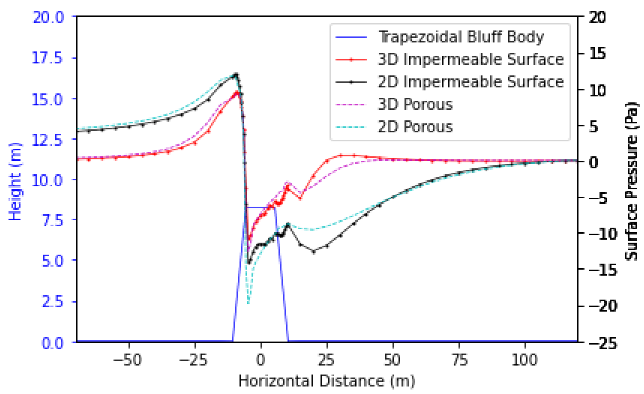

Figure 7 Field-Scale Surface Pressure distributions on a Trapezoidal Bluff Body for 2D and 3D, porous and surface only models for an inlet velocity of 5 m·s^{-1}. Flow here moves from left to right.

Here we can see that the same general patterns remain the same, with the high-pressure spike at the front of the object, the low-pressure spike as it crests the top of the shape, then a neutral pressure zone towards the back of the shape. We also see that the 2D models have higher pressure spikes than the 3D models, similarly to the previous models for the same reason. However, we can see that the porous models have a higher magnitude in the pressure spikes compared to the impermeable models (approx. 7 to 20 %) in the respective 2D and 3D models, which is opposite to the expected results. The reason for this maybe be due to the y+ value of the field scale models being higher compared to the lab scale models, causing a less accurate representation of the flow separation behaviour. This will require further investigation.

5. CONCLUSION

In conclusion, the numerical modelling done for the flow of wind over the bluff bodies showed that there may be a difference between the behaviour of flow separation over a porous media when it is modelled as a surface only model (two-step method) or when it is modelled as a porous media using a momentum sink approach. The values in the differences between the main pressure spike at the front of each shape (approx. 7-30% difference) indicate that there could be significant differences in modelling porous media as a two-stage modelling approach compared to the momentum sink approach shown here. The experimental investigation can now be used to test the differences between the two model types and be used to calibrate and validate the models.

Pressure gradients at the typical wind speed of 5 $m \cdot s^{-1}$ (and higher) may drive significant exchange within the bedform and external environment. Upscaling from the lab scale to a real-world scale that shows similar pressure gradients as the lab scales may indicate that this process could be a significant driver of exchange in real-world landfills.

Future work will focus on looking at more complicated landfill geometries that may occur in a real landfill, such as various transitions from concave to convex landforms throughout the operational phase of a landfill. In addition to this, the experimental investigation can now be used to test the differences between the two model types and be used to calibrate and validate the models.

REFERENCES

Australian Bureau of Statistics (2020). Waste Account, Australia, Experimental Estimates – Waste generation, management and economic response by industry and household in alignment with System of Environmental-Economic Accounts (SEEA). Retrieved from https://www.abs.gov.au/statistics/environment/environmental-management/waste-account-australia-experimental-estimates/latest-release#:~:text=produced%20by%20DAWE.-,Generation%20and%20management,disposal%20(20.5%20million%20tonnes)

Bayani Cardenas, M., & Wilson, J. L. (2006). The influence of ambient groundwater discharge on exchange zones induced by current-bedform interactions. *Journal of hydrology (Amsterdam), 331*(1-2), 103-109. doi:10.1016/j.jhydrol.2006.05.012

ClimateWatch. (2021). Historical GHG Emissions. Retrieved from https://www.climatewatchdata.org/ghg-emissions?apcid=000000000000000000000000&breakBy=sector&chartType=line&end_year=2021&start_year=1990

Gibbes, B. (2007). Pore water exchange processes in offshore intertidal sandbanks. In. St. Lucia, Qld.: The University of Queensland, School of Engineering.

IPCC. (2021). *Climate Change 2021: The Physical Science Basis. Contribution of Working Group I to the Sixth Assessment Report of the Intergovernmental Panel on Climate Change*. Retrieved from https://www.ipcc.ch/report/ar6/wg1/

Jin, G., Tang, H., Gibbes, B., Li, L., Barry, D. A., Fleckenstein, J. H., . . . Krause, S. (2010). Transport of nonsorbing solutes in a streambed with periodic bedforms. *Advances in water resources, 33*(11), 1402-1416. doi:10.1016/j.advwatres.2010.09.003

OpenCFD. (2019). DarcyForchheimer Class Reference. Retrieved from https://www.openfoam.com/documentation/guides/v2206/api/classFoam_1_1porosityModels_1_1DarcyForchheimer.html

Pickin, J., & Macklin, J. (2025). *National waste and resource recovery report 2024*. Retrieved from https://www.dcceew.gov.au/sites/default/files/documents/national-waste-and-resource-recovery-report-2024.pdf

